Frindy, S.; Primo Arnau, AM.; Lahcini, M.; Bousmina, M.; García Gómez, H.; El Kadib, A. (2015). Pd embedded in chitosan microspheres as tunable soft-materials for Sonogashira cross-coupling in water-ethanol mixture. Green Chemistry. 17(3):1893-1898. doi:10.1039/c4gc02175d.

Pd Embedded in Chitosan Microspheres as Tunable Soft-Materials for Sonogashira Cross-Coupling in Water-Ethanol Mixture

Sana Frindy,[a,b] Ana Primo,[b] Mohamed Lahcini,[a] Mosto Bousmina,[c,d] Hermenegildo Garcia,[b] Abdelkrim El Kadib.[c,*]

Received (in XXX, XXX) Xth XXXXXXXXX 20XX, Accepted Xth XXXXXXXXX 20XX
DOI: 10.1039/b000000x

Easy shaping of chitosan (CS) as porous self-standing nanofibrillar microspheres allows their use as palladium carrier. Amino-groups on CS enables Pd coordination to be modulated, given rise to three different support-catalyst interactions: weakly-coordinated Pd-CS in native CS, incarcerated Pd-CS-Glu in cross-linked CS and strongly-ligated Pd-CS-SH, attained by introduction of thiol arms in CS. These catalysts efficiently promote under mild and sustainable conditions (water-ethanol as solvent at 65°C) Sonogashira cross-coupling of a large library of functional substrates and stand as recyclable, metal-scavenging catalytic systems.

The attribution in 2010 of the prestigeous Nobel prize to the laureates of cross-coupling catalysis reflects the importance of these pionnering works as landmark in organic chemistry and their strong impact on material science.[1] Since their discovery, these reactions have been widely used in organic synthesis, palladium being recognised as the most active metal and applicable catalyst for a broad range of organic transformations.[2] The high cost of palladium complexes has stimulated the search for alternative more affordable transition metal catalysts including copper and iron, to name a few[3] and even, lastly, to the more sustainable metal-free cross-coupling catalysis.[4] While this approach in homogeneous catalysis seems promising, another strategy to reduce these limitations consists on the entrapment or strong coordination of palladium complexes (and their reactive nanosized particles) in heterogeneous porous supports.[5] This enables an easy recovery from the reaction mixture and palladium recycling. Although the "true" heterogeneous nature of these Pd-coupling catalysts is still questionable, as many of them have proven to act as a "release and catch catalytic system",[6] this immobilization principally minimizes the amount of residual toxic metal in the final products, which is another key issue complicating homogeneous Pd catalysis applied to the synthesis of pharmaceuticals.[7] Indeed, a large library of inorganic and organic supports have been already evaluated, including charcoal, inorganic silica, alumina and synthetic polystyrene. Mesoporous silicas for instance present some advantages, such as high surface area, modulable pore diameter and broad possibilities for surface functionalization. However, the unambiguously established instability of the porous system in aqueous and basic conditions, necessary for cross-coupling catalysis, constitutes serious setbacks of these supports.[8] Additionally, the preparation of most mesoporous metal oxides is energy-consuming and time-demanding making investigations on easily accessible and/or available renewable materials appealing as possible alternative supports. In this context, polysaccharides are the most important family of bioresources with enormous potential to provide directly or upon functionalisation, a remarkable variety of well-designed, macromolecular materials. Among them, chitosan (**CS**, a by product of fishing industry) displays the dual feature of being easily physically moldable (to provide porous open framework hydrogels) and chemically modulable (owing to the presence of amino groups amenable to undergo a set of chemical modifications).[9] **CS** hydrogels were recently reported to be efficient medium for the controlling-growth of the transient sol-gel species allowing to generate porous hybrid materials[10,11] and an ideal fibrillar confined microspace to stabilize smaller nano-objects and metallic particles.[12] Moreover, CO_2 supercritical drying of these microspheres has been found to be a reliable procedure to ensure drying without structural or textural alteration from the solvated state (dispersed hydrogel and alcogel) to light-weight aerogel.[10,13] Beside, CS graphitization offers sustainable access to *N*-doped graphene-based materials.[14]

In this contribution, three differents types of CS-based hydrogel microspheres were designed (native **CS** one, their cross-linked analogues **CS-Glu** and the thiolated chitosan **CS-SH**) and used as porous carrier for supporting homogeneous $Pd(OAc)_2$. The rationale behind this selection was to increase the thermal and mechanical stability of CS microspheres by cross-linking (case of **CS-Glu**) and to increase the affinity of CS for Pd^{2+} (case of **CS-SH**) compared to the native **CS**. The resulting supported Pd-containing CS microspheres were then evaluated for Sonogashira cross-coupling catalysis including the synthesis of some relevant pharmaceutical precursors. The catalytic behavior of hydrogels *versus* CO_2 dried aerogels was studied in terms of their kinetics, recovery, recycling and catalytic stability against metal leaching.

Briefly, **CS** microspheres were prepared by introducing single droplets of soluble CS acidic solution - *via* a 0.8 mm needle - into a 0.1 N NaOH aqueous solution. Self-standing hydrogel microspheres in which 2% of the polymer is dispersed in 98% water were immediatly formed. Extensive washing until pH ~ 7 affords the targeted neutral hydrogels. Their immersion in ethanol:water solutions of increased ethanol ratio up to 100% ethanol provides alcogels and their CO_2 supercritical drying enables access to chitosan aerogels. From these **CS** soft alcogel microspheres, two other functional materials have been prepared (Figure 1). Indeed, the amino groups belonging to the chitosan backbone react with glutaraldehyde to yield cross-linked chitosan microspheres **CS-Glu**.[15] Additionally, another fonctionalised CS containing thiol has been prepared by the

ring opening of ɤ-thiobutyrolactone induced by nucleophilic addition of the amino groups[16] given rise to novel 4-mercapto-*N*-butanamide functionalized chitosan (**CS-SH**). The success of these modifications has been ascertained by DRIFT spectroscopy, ^{13}C CP MAS NMR analyses and comparison with literature data of similar fragments.[15,16] In **CS-Glu**, the microspheres turned yellow upon reaction with glutaradehyde *n*(NH_2/Glu) = 1 indicating the spontaneous imine (C=N) formation (S2a, SI). This has been confirmed by DRIFT where the typical signal of primary amine at 1592 cm^{-1} significantly decreases at the expense of new band at 1638 cm^{-1} due to (C=N) vibration (S3, SI). ^{13}C MAS NMR spectroscopy reveals the existence of additional peaks with respect to those of native chitosan (signals around 27.9, 43.6 and 96.7 ppm can be respectively attributed to central CH_2-CH_2-CH_2, the CH_2-CH_2-HC=N and the carbon directly attached to nitrogen atom (C=N)) (S4, SI). In the case of **CS-SH** material, carbon signals of the grafted thiol overlaps with those of native chitosan. However, a new signal observed at 36 ppm has been unambiguously assigned to the CH_2 neighboring SH group (CH_2-SH)[16] (S4, SI). Notably, neither textural, morphological alteration nor visible macroscopic damage of the microspheres have been observed after functionalization.

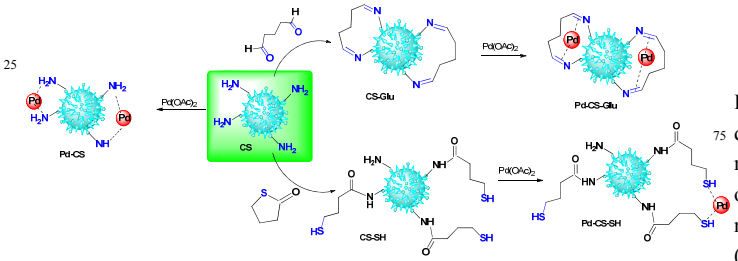

Figure 1. Multi-step preparation of the three chitosan-based catalysts **Pd-CS**, **Pd-CS-Glu** and **Pd-CS-SH** studied in the present work.

Lastly, the ability of these porous hydrogels to scavenge Pd^{2+} complexes has been assessed. Upon immersion in $Pd(OAc)_2$ ethanol solution (ratio NH_2:Pd = 4), the initial orange solution turned clear while the microspheres become black (in the case of **CS** and **CS-Glu**) or orange (in the case of **CS-SH)** (see Figure 2a-b and S2b, SI). This indicates that within native CS and the cross-linked one, Pd nanoparticles (naked Pd^0) are formed from Pd^{2+} in the presence of ethanol and both amine/imines as gentle reducing agents, whereas the strong coordination of thiol-to-Pd in **CS-SH** enables stabilization of Pd^{2+}, reminiscent of Pd^{2+} ligation by the ubiquitously used mercaptopropyltrimethoxysilane-tethered silica.[17]

Gratifyingly, CO_2 supercritical drying allows avoiding the gel shrinkage that may occur during solvent evaporation due to the capillary forces exerted on the soft-material walls. Consequently, **Pd-CS** and **Pd-CS-Glu** aerogels exhibit specific surface area of 239 $m^2.g^{-1}$ as mesured by nitrogen sorption while the area of **Pd-CS-SH** aerogel is slightly larger reaching 302 $m^2.g^{-1}$ (Table 1). This specific surface area enhancement can be tentatively attributed to the weaker hydrogen-bonding forces among the fibrils of the biopolymer upon thiol grafting. The hydrogen-bonding network stores polar water and ethanol within the microspheres and are responsible for the slight shrinkage (~5%) that routinely occurs during the gel drying. Expectedly, examination of the cross-section microspheres by scanning electron microscopy reveals the presence of entangled fibrillar network with a void space exeeding 500 nm, typical of the macroporosity generated during **CS** gelation (Figure 2c-d and S5, SI). Nanosized palladium particles have been observed by TEM analysis (average diameter ~ 5 nm) for **Pd-CS** pointing to the efficacy of CS to limit the Ostwald-ripening growth of palladium (Figure 2f and S6, SI). ICP analysis enables to estimate the amount of palladium content within the three porous microspheres (Table 1).

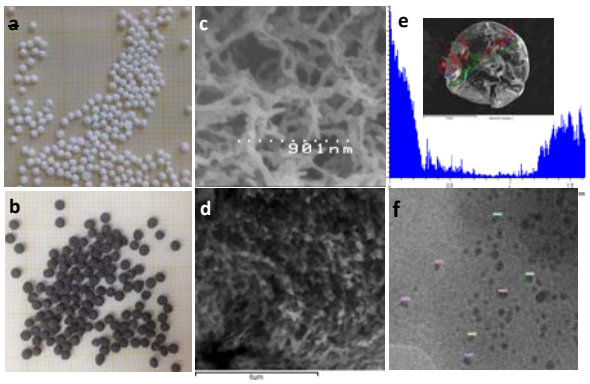

Figure 2. Representative **Pd-CS** images at different magnification : a. digital photos of native **CS** chitosan aerogels. b. black **Pd-CS** microspheres (scale bar: each small square is equal to 1 mm^2). c. SEM of native **CS** showing fibrillar opened porous network (scale bar : 901 nm). d. SEM of **Pd-CS** evidencing that the initial network is preserved (scale bar: 6 µm). e. palladium distribution mapped by EDX analysis along the cross-section microsphere. f. TEM analysis evidencing the presence of palladium nanoparticles inside of the biopolymer.

Table 1. Specific surface areas, palladium content and leached palladium during catalysis.

Material	[a] S_{BET}	[b] Pd (wt%)	[c] Leached Pd %
Pd-CS	239	13.89	0.014
Pd-CS-Glu	239	13.10	0.029
Pd-CS-SH	302	17.49	0.022

[a] measured by nitrogen sorption analysis. [b] measured by ICP analysis. [c] residual palladium in solution after Sonogashira cross-coupling of 4-iodo-acetophenone to phenylacetylene.

The highest Pd content (17.49 wt%) is obtained for **CS-SH** in consistency with the higher affinity of thiol groups for palladium. Native chitosan **CS** contains 13.89 wt% Pd whereas the cross-linked **CS-Glu** has slightly lower Pd content of 13.10 wt%, being the lowest value uptake of palladium. To accuratly establish the chemical structure of the palladium hosted within the microspheres, the three grinded aerogels were analysed by X-ray photo-electron spectroscopy (XPS: (setting reference C_{1s}= 284.5 eV)). Pd $3d_{3/2,5/2}$ binding energy indicates that the metal ligated to **CS-SH** corresponds to Pd^{+2} (340 eV for $3d_{5/2}$ and 345 eV for $3d_{3/2}$) with virtually no Pd^0 observed (S7, SI). In

Pd-CS microspheres, similar binding energies are observed with an additional minor peak at 338 eV that typically suggests the presence of a fraction of reduced Pd^0 (S7, SI). In sharp contrast, **Pd-CS-Glu** microspheres features two palladium species; the most abundant one being Pd^0 with its binding energy at 337 eV and 343 eV and those of Pd^{+2} at 340 and 346 eV for $3d_{5/2}$ and $3d_{3/2}$ respectively (S7, SI).[18,19]

At this point, three Pd-hosted alcogel- and aerogel-based materials with similarities in their intrinsic textural properties of the support (macroporous fibrillar network and millimetric dimension of the microspheres), but with different metal-support coordination strength (weakly coordinated Pd in **CS**, incarcerated Pd nanoparticles in **CS-Glu** and strongly coordinated Pd^{2+} in **CS-SH**) were prepared. Beside our motivation to elucidate - for the first time - the difference on the performance of support in catalysis between **CS** alcogels and aerogels, a second important point is to determine how **CS** functionalization influences the catalytic activity and if there is a borderline between efficient scavenger and efficient catalyst. To address thes issues, Sonogashira cross-coupling of aryl iodide and acetylene derivatives was selected as a prototypical reaction. With some guidelines of sustainable chemistry in mind, solvents like dimethylformamide and toluene, organic bases like NEt_3, harsh temperatures and the presence of copper as a second metal were all discarded. Under milder conditions (EtOH-water as solvent, K_2CO_3 as base, T = 65 °C) and regardless of the alcogel used, 4-iodoacetophenone coupled to phenylacetylene affording selectively, after 6 h, a quantitative yield of the targeted product **1**.

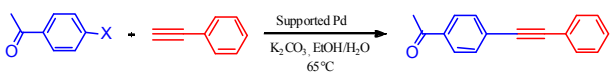

At the end of the reaction, the catalyst is easily recovered by simple removal of the microspheres even without the need of filtration making very simple the work-up procedure related to the catalyst removal.

Kinetic investigations have been performed aiming to get a better understanding on the catalytic behavior of these microspheres depending on the nature of the support (wetted gel *versus* CO_2-dried aerogels) and that of the support-metal interaction (weakly-coordinated, incarcerated nanoparticles or strongly-chelated). Indeed, for the three materials, dried aerogels were found to be more active than their alcogel analogues (Figure 3). Δ_{conv} $(t = 1h) = Conv_{aerogel} - Conv_{alcogel}$ calculated for the three materials reveals the highest value of 43.54 for **Pd-CS-Glu**, 23.34 for **Pd-CS** and 14.59 for **Pd-CS-SH**. A plausible explanation can be the difference in swelling wetted *versus* dried microspheres, a phenomenon that may impact the adsorption and desorption of the reactants and products respectively, to- and from- active catalytic sites. In this context, several discrepancies have been previsouly reported between hydrogels and dried aerogels with regard to their interaction with molecular species (different diffusion rates during the sol-gel process,[20] different selectivities in organic synthesis,[21,22] different viscosities, variable storage capacities for water).

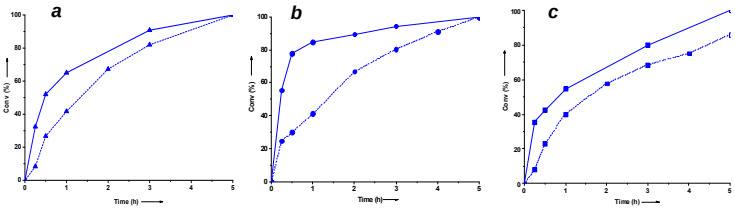

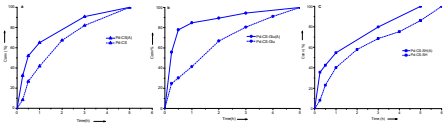

Figure 3. Catalytic activity of alcogels versus aerogels in cross-coupling of 4-bromoacetophenone to phenylacetylene. a. **Pd-CS**. b. **Pd-CS-Glu**. c. **Pd-CS-SH**. Dashed lines correspond to alcogels and normal lines to aerogels.

Plotting the activity with respect to the nature of functional groups revealed - for both alcogels and aerogels - inferior catalytic activity for **Pd-CS-SH** compared to **Pd-CS** and **Pd-CS-Glu** (S8c-d). TOF (h^{-1}) was found to decrease from 25.84 for **Pd-CS-Glu** to 17.43 for **Pd-CS** to 14.2 for **Pd-CS-SH** for aeorgels. Similar trend was observed for alcogels with TOF (h^{-1}) values decreasing from 9.55 for **Pd-CS-Glu** to 8.28 for **Pd-CS** to 6.66 for **Pd-CS-SH**. This activity order suggests that Pd nanoparticles are active sites promoting the coupling, as it is known in the literature, with higher efficiency than Pd^{2+} ligated. The catalytic activity ranking seems in agrement with XPS analysis from which it has been concluded that **Pd-CS-Glu** features the highest proportion of palladium nanoparticles, compared to **Pd-CS** and **Pd-CS-SH**. At the end of the reaction, however, XPS investigation on the recovered **Pd-CS-SH** reveals four binding sites assignable to Pd^0 (338.2 and 343.2 eV) and Pd^{+2} (341.1 and 346.2 eV). This result indicates that some Pd^{+2} species escape the strong thiol ligation during catalysis and are subsequently converted to naked Pd^0. ICP analysis performed on the cross-coupling reactions after cooling of the resulting solutions enabled quantification of leached palladium catalyst from the three CS-based catalyst. Whatever the material used, only tiny amount of palladium is released in the solution : 0.014% for **Pd-CS**, 0.029% for **Pd-CS-Glu** and 0.022% for **Pd-CS-SH** (Table 1). In the three cases, more than 99.97% of the Pd initially present in the catalyst is retained within the microspheres. The absence of significant leaching is of particular interest given numerous precedents on the occurrence of palladium leaching during Sonogashira cross-coupling. This fact is attributed to the strong coordination of palladium to the alkyne functionality either of the product or the starting material.[7,23] Herein and given their low metal contamination, the obtained products do not need additional scavening to meet regulatory specifications.

Without any chemical or thermal activation, these soft-supported catalysts can be reused – after simple washing with ethanol- five additional runs, while maintaining their activity (Figure 4). After that, whereas **Pd-CS** and **Pd-CS-Glu** preserve their initial shape allowing more extended reuse in catalysis (to reach 6 runs), **Pd-CS-SH** dissolves to a slurry form and under these circumstances, the catalyst recovery and its further reuse become extremely difficult. The low morphological stability of **Pd-CS-SH** microspheres can be explained by the weakening of hydrogen bonding at the fibrillar level, as a result of amine fuctionalisation (that are normally engaged in NH_2---HO bonding), in contrast to those occurring in the pristine, non-functionalized CS microspheres. In the case of **CS-Glu**,

although hydrogen-bonding network is disrupted, the chemical cross-linking of the chains considerably improves the r

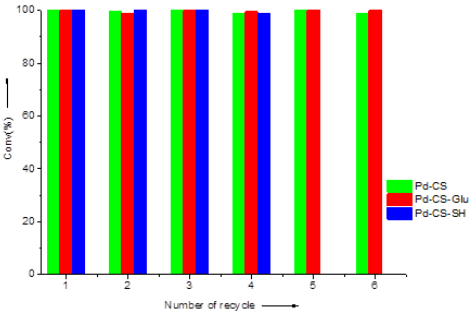

Figure 4. Recycling of the three Pd supported on CS and modified CS alcogel catalysts in the Sonogahsira coupling of 4-iodoacetophenone with phenylacetylene.

Table 2. Extending the scope of Sonogashira cross-coupling to other alkyne and halide substrates.

Entry	Arylhalide	Alkyne	Catalyst	Time	Product	Yield
1	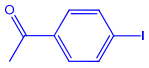	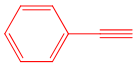	**Pd-CS** 3%	6h	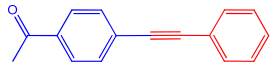	98%
2	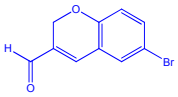	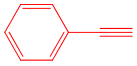	**Pd-CS-Glu** 1%	6h	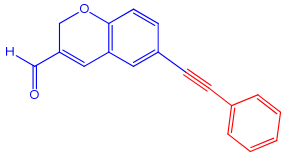	52%
3	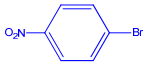	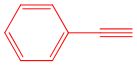	**Pd-CS** 0.1%	8h	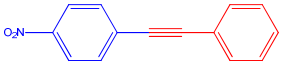	100%
4	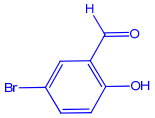	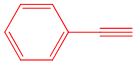	**Pd-CS-Glu** 1%	20h	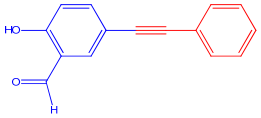	100%
5	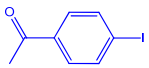	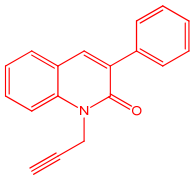	**Pd-CS-SH** 3%	8h	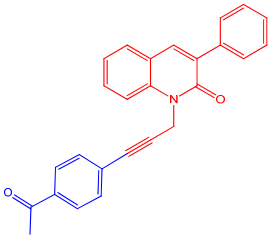	96%
6	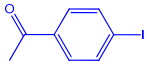	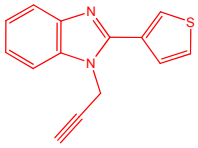	**Pd-CS-SH** 3%	8h	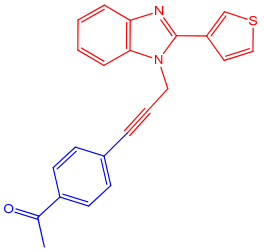	72%

Prompted by these promising results, we subjected these catalysts to more demanding, challenging and/or prevalent coupling catalysis. With phenylacetylene as substrate, three aryl bromides were successfully coupled using tiny amounts of supported Pd (0.1 to 3% of either **Pd-CS**, **Pd-CS-Glu** or **Pd-CS-SH**) under the previously described conditions yielding the targeted alkynes in good to quantitative yield (Entries 2 to 4, Table 2). Heterocycles with biological activity and terminal propargylic fragment were also tested for Sonogashira cross-coupling in the presence of 4-iodoacetophenone as starting halide (Entries 5 and 6, Table 2). The efficacy of these catalysts enables to obtain, with a simple work-up, the targeted coupling products in 72% and 96%, respectively.

To sum up, this work highlights the multifaceted advantages of CS as sustainable material for textural enginnering of macroporous supports, while chemical modification of its

amino groups allows tuning the metal-support interaction. Mild and sustainable reaction conditions (copper-free, ethanol-water as solvent, 65 °C) enable Sonogashira cross-coupling catalysis to be performed with quantitative yields, low metal contamination, easy work up and good recyclability. This straightforward and sustainable chemistry affords versatile eco-efficient catalysts bearing many useful properties: their gentle reducing conditions to produce metal nanoparticles (without using toxic reducing agents neither hydrogen treatment) and their easy recovery from the reaction medium whereas heterogeneous system needs specific filters are among their most illustrative advantages over the existing Pd-supported catalysts. The metal scavenging ability of these microspheres can be interesting for the synthesis of active pharmaceutical ingredients, specifically those for which the metal contamination has to be reduced to few ppb.

We are indebted to Dr. Rachid Bouhfid for the donation of the starting propargylic derivatives. S.F. is thankful to the EMMAG-Erasmus mundus program for funding. UEMF is warmly acknowledged for the financial support.

[a] *Laboratory of Organometallic and Macromolecular Chemistry - Composites Materials, Faculty of Sciences and Technologies, Cadi Ayyad University, Avenue Abdelkrim Elkhattabi, B.P. 549, 40000 Marrakech, Morocco*

[b] *Instituto de Tecnologia Quimica CSIC-UPV and Departamento de Quimica. Univ. Politicnica de Valencia, Av. de los Naranjos s/n 46022 Valencia (Spain).*

[c] *Euro-Med Research Institute. Engineering Division. Euro-Mediterranean University of Fes (UEMF), Fès-Shore, Route de Sidi Hrazem, 30070 Fès (Morocco). E-mail: a.elkadib@ueuromed.org*

[d] *Hassan II Academy of Science and Technology, Avenue Mohammed VI, 10222 Rabat, Morocco.*

† Electronic Supplementary Information (ESI) available: [Synthesis and characterizations of precursors and materials]. See DOI: 10.1039/b000000x/

1 C. C. C. Johansson Seechurn, M. O. Kitching, T. J. Colacot, V. Snieckus, *Angew. Chem. Int. Ed.*, **2012**, *51*, 5062–5085.

2 P. Sehnal, J. K. R. Taylor, I. J. S. Fairlamb, *Chem. Rev*., **2010**, *110*, 824-889. C. Torborg, M. Beller, *Adv. Synth. Catal*., **2009**, *351*, 3027-3043. J. F. Hartwig, *Nature*, **2008**, *455*, 314-322.

3 R. Loska, M. R. C. Volla, P. Vogel, *Adv. Synth. Catal*., **2008**, *350*, 859-2864. C. L. Sun, B. J. Li, Z. J. Shi, *Chem. Rev*., **2011**, *111*, 1293-1314. W. M. Czaplik, M. Mayer, J. Cvengros, *ChemSusChem*, **2009**, *2*, 396-417. A. Furstner, A. Leitner, M. Mendez, *J. Am. Chem. Soc*., **2002**, *124*, 13856-13863.

4 J. Barluenga, C. Valdes, *Angew. Chem. Int. Ed*., **2011**, *50*, 7486-7500.

5 Y. Lunxiang, L. Jürgen, *Chem. Rev*., **2007**, *107*, 133–173.

6 N. T. S. Phan, M. V. D. Sluys, C. W. Jones, *Adv. Synth. Catal.*, **2006**, *348*, 609–679. M. Weck and C. W. Jones, *Inorg. Chem*., **2007**, 46 (6), pp 1865–1875. J. D. Webb, S. MacQuarrie, K. McEleney, C. M. Crudden, *J. Catal.*, **2007**, *252*, 97-109.

7 C. E. Garett, K. Prasad, *Adv. Synth. Catal*., **2004**, *346*, 889.

8 B. W. Glasspoole, J. D. Webb, C. M. Crudden, *J. Catal.*, **2009**, *265*, 148-154. A. Modak, J. Mondal, A. Bhaumik, *Green Chem*., **2012**, *14*, 2840-2855.

9 D. J. Macquarrie and J. J. E. Hardy, *Ind. Eng. Chem. Res*., **2005**, *44*, 8499–8520. A. El Kadib, *ChemSusChem*, DOI: 10.1002/cssc.201402718.

10 A. El Kadib, A. Primo, K. Molvinger, M. Bousmina, D. Brunel, *Chem. Eur. J.*, **2011**, *17*, 7940 – 7946.

11 A. El Kadib, M. Bousmina, *Chem. Eur. J.*, **2012**, *18*, 8264-8277.

12 A. El Kadib. M. Bousmina, D. Brunel, *J. Nanosci. Nanotechnol.*, **2014**, *14*, 308-331. A. Primo, F. Quignard, *Chem. Comm*., **2010**, *46*, 5593-5595.

13 R. Valentin, K. Molvinger, F. Quignard, D. Brunel, *New. J Chem.*, **2003**, *27*, 1690.

14 A. Primo, P. Atienzar, E. Sanchez, J. M. Delgado, H. García, *Chem. Commun*., **2012**,48, 9254-9256.

15 W.S.Wan Ngah, S. Ab Ghani, A. Kamari, *Bioresource Technology*, **2005**, *96*, 443–450.

16 S. El Hankari, A. El Kadib, A. Finiels, A. Bouhaouss, J. J. E. Moreau, C. M. Crudden, D. Brunel, P. Hesemann. *Chem. Eur. J.*, **2011**, *17*, 8984-8994.

17 C. M. Crudden, M. Sateesh, R. Lewis *J. Am. Chem. Soc*., **2005**, *127*, 10045–10050

18 For an accurate investigation of heterogeneous Pd-based materials by XPS analysis, see: K. McEleney, C. M. Crudden, J. H. Horton., *J. Phys. Chem.C*, **2009**, *113*, 1901-1907.

19 Similar binding energy was observed for Pd^0 grown in MOF, generated upon treatment in a stream of H_2 at 200°C. See: A. S. Roy, J. Mondal, B. Banerjee, P. Mondal, A. Bhaumik, S. M. Islam, *Appl. Catal. A: Gen*., **2014**, *469*, 320-327.

20 A. El Kadib, K. Molvinger, T. Cacciaguerra, D. Brunel, M. Bousmina. *Micro. Meso. Mater*., **2011**, *142*, 301.

21 D. Kühbeck, G. Saidulu, K. R. Reddy, D. D. Díaz, *Green Chem*., **2012**, *14*, 378-392

22 A. K.-Nezhad, S. Mohammadi, *RSC Adv*., **2014**, *4*, 13782-13787.

23 A. El Kadib, K. McEleney, T. Seki, T. K.Wood, C. M. Crudden, *ChemCatChem*, **2011**, 3, 1281-1285